Shell-wise oxidation of nanocrystalline silicon observed by X-ray diffraction and TEM

Walter Vogel,*[a] Sabina Botti,[b] Stefano Martelli[b] and Elvio Carlino[c]

[a] *Fritz-Haber-Institut der Max-Planck-Gesellschaft, D-14195 Berlin, Germany*
[b] *ENEA, Dip. Innovatione, Settore Fisica Applicata, Centro Ricerche Frascati, P.O. Box 65, I-00044 Frascati, Rome, Italy*
[c] *PASTIS-Centro Nazionale Ricerca e Sviluppo Materiali (PASTIS-CNRSM), S.S. 7 Appia, km. 712, I-72100 Brindisi, Italy*

The oxidation of nanocrystalline silicon powder (average crystallite size of 87 Å), prepared by laser-driven pyrolysis of SiH_4, has been studied by X-ray diffraction and transmission electron microscopy. In a previous study the Si particles were shown to form perfect isolated near-spherical 'single crystals' that are stable up to 1073 K under high vacuum conditions. We have measured the size reduction of the Si nanoparticles in a flow of oxygen as a function of the degree of oxidation. The results are in agreement with model calculations for a shell-wise oxidation of silicon surface layers to amorphous silicon oxide. An oxidation to 50 vol.% implies a size reduction of 20% and tenfold improved visible photoluminescence intensity. Preliminary kinetic studies at 656 K in oxygen indicate a self-limiting type of oxidation, which is reached for an oxide layer thickness of $\approx$6.8 Å

Room temperature photoluminescence (PL) of nano-sized Si has recently gained extensive attention with regard to possible applications in optoelectronic devices.[1–4] By laser-driven pyrolysis of silane, ultra-pure, near-spherical solid Si particles are obtained.[4–6]

Most work in this field has been devoted to electrochemically etched porous Si films. On the other hand, silicon clusters (Si_N) consisting of a few atoms ($N < 100$) have attracted growing attention, among them the fullerene-like Si_{45} clusters.[7] Free-standing nano-sized silicon particles, grown by gas aggregation, offer the possibility of performing size-selective studies, avoiding any particle–substrate interaction. In a recent study it has been shown that these particles are stable under ambient conditions, probably by the formation of a thin passivating surface oxide layer. Moreover, they appear as near perfect 'single crystals' and only 3% of them are twinned.[8]

Surface effects are enhanced with the decreasing size of nanocrystals, due to the increasing surface-to-volume ratios. The surface acts as a source of novel electronic states that play an important role in photoluminescence characteristics.[3,4] A change of PL intensity with Si nanocrystal size has been observed, whereas the position of the PL peak energy scarcely depends on particle diameter.[4] This finding stresses the importance of studying the interfacial region between the crystalline Si core and the oxide layer.

It is also important to study the effect of oxidation on PL features. As for porous silicon, annealing should stabilise the luminescence intensity in time.[1]

The mechanism and kinetics of surface oxide formation has been extensively studied for silicon single crystal surfaces. However, to our knowledge no such study has so far been reported on nanocrystalline silicon. In this work we use X-ray diffraction (XRD) and transmission electron microscopy (TEM) to characterise the structural changes induced by exposure to oxygen as a function of temperature and time.

Experimental

Sample preparation

The silicon nanopowder studied in this work was produced by laser synthesis from a gaseous precursor. Details of the preparation technique are given in a previous paper.[9] By X-ray line profile analysis and TEM measurements the resulting particle shape was found to be near-spherical with a mass-averaged crystallite size of 87 Å.[8]

Oxidation of the nano-Si was performed in a quartz tube oven. Batches of the synthesised material have been exposed in a furnace to a water-saturated oxygen flow (purity 4.9) at different temperatures and times (see Fig. 1) and subsequently studied by XRD.

X-Ray diffraction

X-ray experiments have been conducted with a Guinier counter diffractometer (HUBER), equipped with an *in situ* reaction chamber described elsewhere.[10] A Ge(111) curved

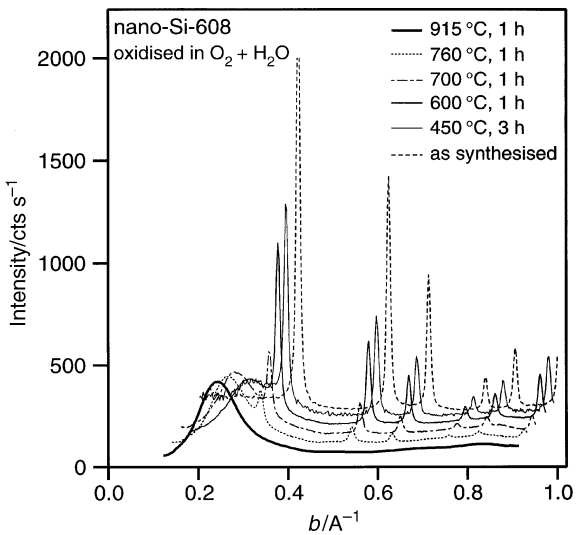

Fig. 1 The background-corrected X-ray diffraction curves are shown with offsets *vs.* the reciprocal scattering length $b = 2 \sin \vartheta/\lambda$ (ϑ: Bragg angle theta; λ: wavelength, $\lambda = 1.5406$ Å). The transformation of c-Si to a-SiO_2 after treatments in $O_2 + H_2O$ at different temperatures is indicated by the gradual depression of the crystalline Bragg peaks and the increase of the amorphous a-SiO_2 halo in the XRD patterns

crystal monochromator (Johanson type) was used to produce a focused Cu-Kα_1 primary beam. For the *in situ* measurements the powder samples were fixed tightly, but not gas tight, between two 0.1 mm Be platelets, separated by a 0.3 mm frame. A K-type thermocouple was placed in the interior of the cuvette. The oxidised samples were pressed into thin self-sustaining pellets and the diffraction patterns were taken *ex situ*.

Electron microscopy

The transmission electron microscopy (TEM) measurements were recorded using a Philips CM30 TEM/STEM operating at 300 kV with a interpretable resolution of 2.3 Å. The specimens for TEM experiments were prepared by depositing the nanocrystalline Si powders onto a copper grid that had been previously covered with a thin carbon film.

Photoluminescence

The PL spectra were obtained at room temperature from as-synthesised and oxidised powders. These samples were excited at $\lambda = 457$ nm and the PL spectra recorded on a PTI spectrofluorimeter with extended red response.

Results and Discussion

Since quantum refinement effects and the surface oxide play a decisive role in the PL of small Si particles, it is important to know the dependence of the mean particle size as a function of the degree of oxidation. This information can be gained from the diffraction patterns.

Fig. 1 shows the sequence of XRD patterns for progressively oxidised nano-Si. The temperature and duration of oxidation are indicated in the figure. The evolution of an amorphous SiO_2 phase (a-SiO_2) is clearly seen from the figure, ending with 100% oxidation at 915 °C. In Fig. 2 we show the intensity curve of as-synthesised Si (top) and then oxidised at 700 °C for 1 h (bottom). The intensity curve of pure a-SiO_2 is fitted as a background curve to the partly oxidised samples (dotted line). The subtracted intensity (thin line) is that of the residual crystalline silicon (c-Si) phase.

We are now able to estimate the mass fraction γ of oxidised Si. Let $\langle I_a \rangle$ be the total intensity of a-SiO_2 scattered in the range $b = 0.1$–1 Å^{-1} that is available to the experiment. Then we have $\langle I_a \rangle \approx \gamma(\langle f^2(\mathrm{Si}) \rangle + 2\langle f^2(\mathrm{O}) \rangle)$, and for the crystalline phase $\langle I_c \rangle \approx (1-\gamma)\langle f^2(\mathrm{Si}) \rangle$, where the fs are the atomic scattering factors. The quotient q of both terms is

$$q = \langle I_a \rangle / \langle I_c \rangle = \gamma(1 + 2p)/(1 - \gamma), \text{ with} \quad (1)$$

$$p = \langle f^2(\mathrm{O}) \rangle / \langle f^2(\mathrm{Si}) \rangle \approx Z^2(\mathrm{O})/Z^2(\mathrm{Si}) = (8/14)^2 \quad (2)$$

For the last approximation we use a 'unified' X-ray atomic scattering factor f_u with $f \approx Zf_u$. The mass fraction of a-SiO_2 is therefore

$$\gamma = q/(1.65 + q) \quad (3)$$

It should be noted that eqn. (3) accounts for the additional intensity contributed by two extra oxygen atoms in a-SiO_2. This can be done for all degrees of oxidation. In the synthesised and air-exposed state the fraction of a-SiO_2 covering the nanocrystalline particles is $\leqslant 6$ vol.%. The related average crystallite sizes are obtained from the integral line width of the peaks in the difference curves.

The kinetics of silicon oxidation has so far only been studied on single crystal surfaces. Surface spectroscopic techniques fail, however, for nanocrystalline materials. In the search for alternatives X-ray diffraction is one of the techniques that becomes surface sensitive for sufficiently small particles.[10] In Fig. 3 we show the development of the amorphous SiO_2 halo intensity and the reversal of the [111] integral intensity of c-Si during *in situ* oxidation. This measurement has been performed at 383 °C in 1 bar of dry oxygen by repeated scans over a range of Bragg angles ($\vartheta = 7$–20 grd; repeat time = 4 min). The data can be renormalised to the volume fraction of oxidised c-Si. For simplicity we assume uniform spherical particles and shell-wise oxidation. Then the linear rate of oxidation dx/dt *vs.* thickness x of the surface layer removed from the crystalline core can be deduced from this graph (insert to Fig. 3). Details of these kinetic studies will be published in a forthcoming paper.

To model the oxidation process, we suggest shell-wise oxidation of spherical particles, having a log normal distribution (LND) in the as-prepared state. The size distribution is modified after several steps of shell removal from the crystalline nuclei as is shown in Fig. 4. Initially, independently of any special size distribution, the relative change of size is pro-

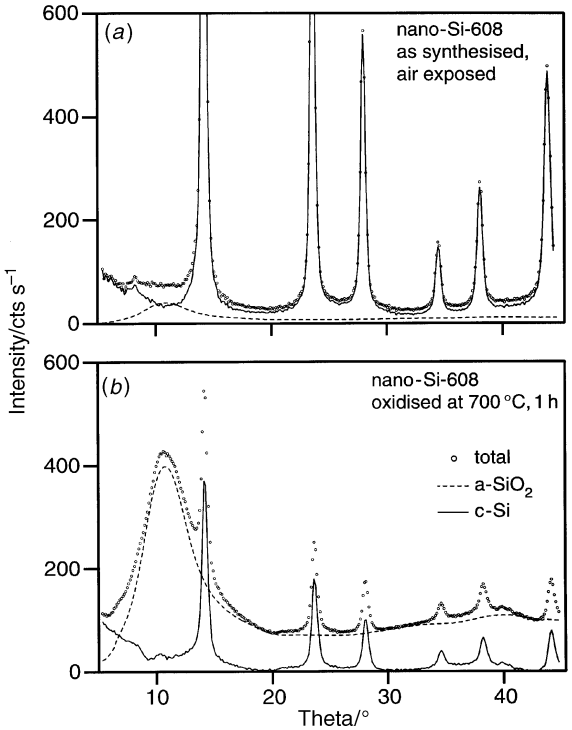

Fig. 2 The intensity fraction of a-SiO_2 (dashed line) that contributes to the total scattered intensity (circles). The difference intensity (solid line) is the diffraction of the crystalline core (c-Si). (*a*) As synthesised and (*b*) oxidised at 700 °C for 1 h

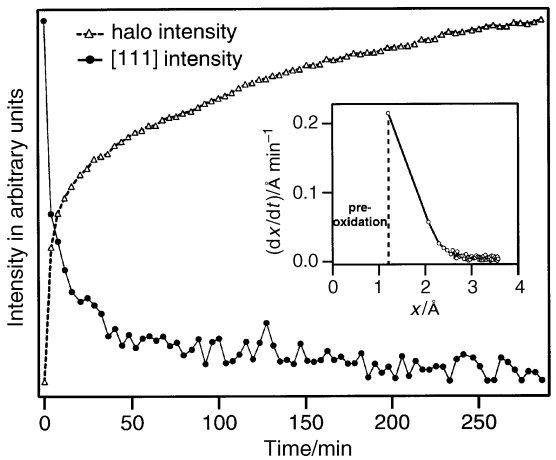

Fig. 3 *In situ* X-ray measurement of the a-SiO_2 halo intensity and the [111] c-Si integral intensity in 1 bar of O_2 at 383 °C. The insert shows the rate of oxidation of c-Si *vs.* the surface layer thickness removed from the c-Si core

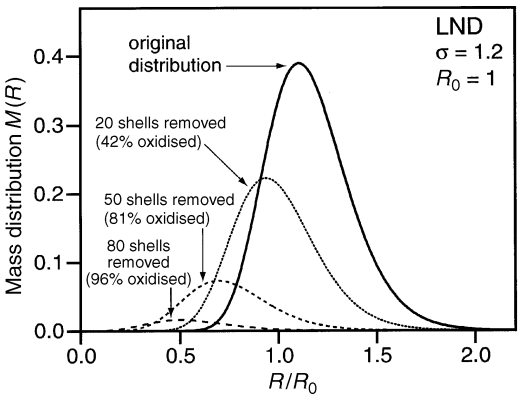

Fig. 4 Mass-weighted log normal size distribution (LND) of spherical particles *vs.* their radii. The distributions are modified as indicated after successive removal of shells of surface layers

portional to one-third of the relative change of the sphere volume.

In Fig. 5 the relative decrease of the mass mean crystalline sphere radius R_M is given as a function of the corresponding relative decrease of total mass M of the crystalline phase. With increasing oxidation the decrease of the mean size depends strongly on the polydispersity of the starting distribution, expressed by the variance σ of the LND. The higher the polydispersity the smaller is the size reduction. The experimental data points are given in the figure and agree well with the proposed model of shell-wise particle oxidation. They fall approximately on a curve with $\sigma = 1.2$. Note that for a reduction of the crystallites to half the size of the starting material a 95% oxidation is needed.

The model correlates with measurements recorded with an electron microscope. Fig. 6 shows high resolution electron microscopy images of nanocrystalline Si heat-treated for one hour in wet oxygen at (*a*) 600 °C and (*b*) 700 °C, respectively. In the central part of Fig. 6(*a*) the crystalline core, (64 ± 4 Å) in diameter, is observed along the [110] zone axis. The crystalline core is surrounded by an amorphous layer, (12 ± 4) Å thick, of silicon oxide. The arrows in Fig. 6(*b*) point to the nanocrystalline Si particles embedded in the amorphous silicon oxide matrix.

The PL spectra recorded at room temperature are shown in Fig. 7 for as-synthesised and annealed powders (oxygen, 600 °C, 1 h). The as-synthesised sample (L = 87 Å) has two bands centred at about 1.5 and 1.7 eV. The effect of annealing is to increase the luminescence intensity by one order of magnitude and to reduce the contribution of the band at higher energy.

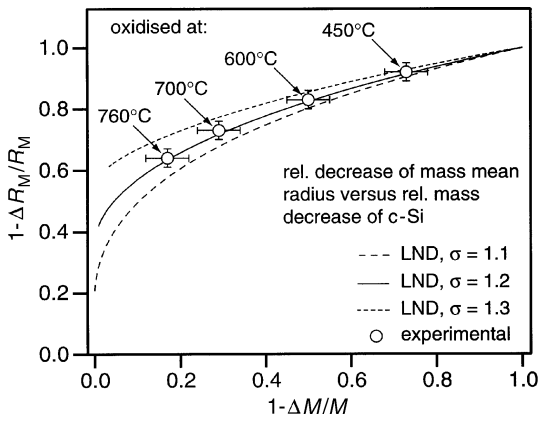

Fig. 5 Relative decrease of the mass mean radius R_M *vs.* the relative decrease of the total mass M for a shell-wise oxidation of spherical particles. The circles are the values for nanocrystalline Si measured by XRD

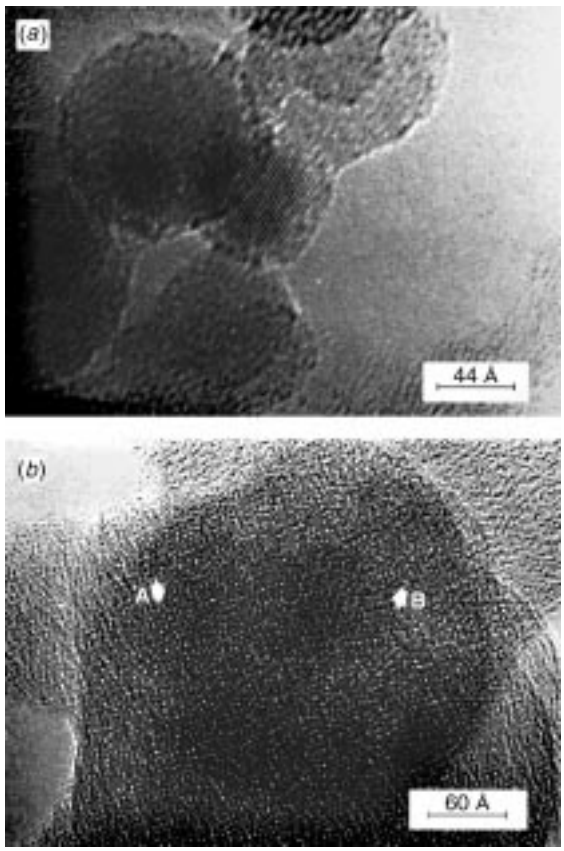

Fig. 6 High resolution transmission electron microscopy images of nanocrystalline Si oxidised for 1 h at (*a*) 600 °C and (*b*) 700 °C. The arrows mark the Si nanocrystalline clusters in the amorphous silicon oxide matrix

According to the three-shell model[4] the characteristics of PL spectra can be explained in the following way: the photogeneration of carriers occurs in the crystalline Si core region and the electrons relax in the lower energy localised state of the near-surface region.

The band gap of surface states depends on the termination of Si particles. *Ab initio* band structure calculations predict that the energy gap of a surface silicon monolayer decreases when increasing the percentage of O-terminated silicon bonds: from about 1.9 eV for 20% oxygen termination (other bonds are H-terminated) to 1.7 eV for fully oxidised silicon sheets.[4] These values roughly agree with the energy peaks of the luminescence spectra.

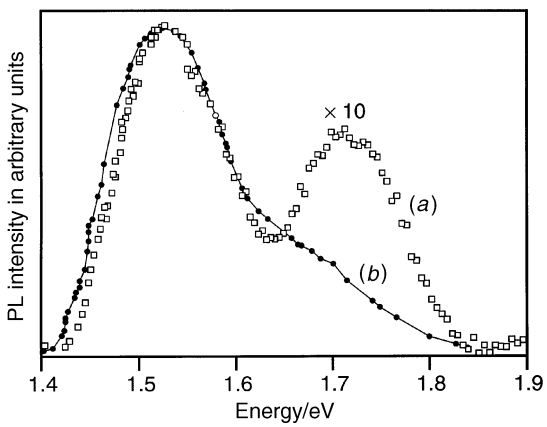

Fig. 7 Luminescence spectra from (curve *a*) the as-synthesised sample and (curve *b*) the sample oxidised for 1 h at 600 °C

By raising the annealing temperature, the percentage of fully oxidised silicon particles becomes more relevant causing, the reduction of the band intensity at higher energy. The increase of PL spectra intensity is due to the reduction of the average dimension of the silicon cores. As a matter of fact, confinement in the interfacial region can be observed only for particles with sizes smaller than 50–80 Å.[4]

Conclusion

Nano-sized silicon particles, prepared in the described manner and having an average size of 87 Å, diffract as near perfect 'single crystals' and only 3% are twinned.[8] Vacuum treatment up to 800 °C does not induce particle growth. The reason for this high stability may be either (*i*) hydrogen termination of the surface dangling bonds or (*ii*) surface coverage by a thin oxide layer, but can not be affirmed at present.

We conclude that the synthesised and air-exposed nano-silicon particles of the present work are covered by a thin a-SiO_2 film. The oxide volume fraction is $\approx 6\%$. For a spherical shell ΔR on top of a sphere of radius $R = 58$ Å the volume fraction $\Delta V/V = 3\Delta R/R = 6\%$ is related to $\Delta R \approx 1$ Å. This means that on average only one monolayer of the nano-Si surface would be oxidised under ambient conditions.

Although X-ray diffraction and HREM confirm the validity of the proposed oxidation model, surface oxidation does not appear to be an effective and valuable method for obtaining very small c-Si particles: a reduction of the mean particle size by more than half of its original value would require near complete oxidation. However, the visible photoluminescence intensity of the nanocrystalline silicon is amplified by one order of magnitude after a 1 h exposure to oxygen at 600 °C, corresponding to a volume fraction oxidised of $\approx 50\%$ and a reduction of the average crystallite size by $\approx 20\%$.

Preliminary kinetic studies at 383 °C show a linear decrease of the initial rate of oxidation, starting with $dx/dt \approx 0.2$ Å min^{-1}. The oxidation is self-limiting, since the rate drops to 2.5×10^{-3} Å min^{-1} after a surface layer of ≈ 3 Å thickness has been transformed to a-SiO_2. The corresponding oxide layer thickness is $3 \times 2.27 = 6.8$ Å. Nanostructured silicon devices are of basic future importance for microelectronic devices and the understanding of their oxidation behavior will be essential.

References

1 L. T. Canham, *Appl. Phys. Lett*., 1990, **57**, 1046.
2 H. Takagi, H. Ogawa, Y. Yamazaki, A. Ishizaki and T. Nakagiri, *Appl. Phys. Lett*., 1990, **56**, 2379.
3 Y. Kanemitsu, T. Ogawa, K. Shiraishi and K. Takeda, *Phys. Rev. B*, 1993, **48**, 4883.
4 (a) Y. Kanemitsu, *Phys. Rev. B*, 1994, **49**, 845. (b) Y. Kanemitsu, *J. Lumin*., 1996, **70**, 333 and references therein.
5 S. Botti, A. Celeste and R. Coppola, *J. Appl. Organomet. Chem*., in press.
6 M. Ehbrecht, H. Ferkel, F. Huisken, Y. N. Polivanov, V. V. Smirnov, O. H. Stelmakh and R. Schmidt, *J. Appl. Phys*., 1995, **78**, 5302.
7 M. Menon and K. R. Subbaswamy, *Phys. Rev. B*, 1995, **51**, 17952.
8 W. Vogel, S. Botti and S. Martelli, *J. Mater. Sci. Lett*., 1998, **17**, 527.
9 E. Borsella, S. Botti, M. Cremona, S. Martelli and A. Nesterenko, *J. Mater. Sci. Lett*., 1997, **16**, 221.
10 N. Hartmann, R. Imbihl and W. Vogel, *Catal. Lett*., 1994, **28**, 373.

Received in Montpellier, France, 21*st October* 1997;
Paper 7/09239C